Electronic Supplementary Information (ESI) for Dalton Transactions.

This journal is © The Royal Society of Chemistry 2020

Supporting Information For

Acetoxy functionalized Al(III) based metal-organic framework showing selective "turn on" detection of perborate in environmental samples

*Soutick Nandi,[a] Helge Reinsch,[b] and Shyam Biswas[a]**

[a] Department of Chemistry, Indian Institute of Technology Guwahati, Guwahati, 781039 Assam, India.

[b] Institut für Anorganische Chemie, Christian-Albrechts-Universität, Max-Eyth-Strasse 2, 24118 Kiel, Germany.

** Corresponding author. Tel: 91-3612583309, Fax: 91-3612582349.*

E-mail address: sbiswas@iitg.ac.in.

Materials and Characterization Methods. The ligand 5-acetoxy isophthalic acid (H_2IPA-$OCOCH_3$) was achieved by following the previously reported procedure, which is followed for the preparation of 2,5-diacetoxy benzene-1,4-dicarboxylic acid ligand (Scheme S1).[1] The ^{1}H NMR, ^{13}C NMR and mass spectra of this ligand are shown in Figures S1-S3 (Supporting Information). All other required chemicals were purchased from commercial sources and used without purification. Fourier transform infrared (FT-IR) spectra were recorded with a Perkin Elmer Spectrum two FT-IR spectrometer in the range of 440-4000 cm^{-1} with KBr pellet. The below mentioned indications were employed for the characterization of the absorption bands: medium (m), weak (w), broad (br), very strong (vs), strong (s) and shoulder (sh). Ambient temperature X-Ray powder diffraction (XRPD) patterns were collected on a Bruker D2 Phaser X-ray diffractometer (30 kV, 10 mA) using Cu-*K*α (λ = 1.5406 Å) radiation. FE-SEM images were captured with a Zeiss (Zemini) scanning electron microscope. Thermogravimetric analyses (TGA) were collected under air atmosphere at a heating rate of 10 °C min^{-1} in a temperature region of 25-800 °C by employing a Netzsch STA-409CD thermal analyzer. Fluorescence emission behavior was recorded by a HORIBA JOBIN YVON Fluoromax-4 spectrofluorometer. The excitation wavelength (λ_{ex}) was 365 nm for all the fluorescence experiments. The nitrogen sorption isotherms were performed employing a Quantachrome Autosorb iQ-MP gas sorption analyzer at -196 °C. Prior to the sorption measurement, degassing of the material was performed at 90 °C for 12 h under dynamic vacuum. A Bruker Avance III 600 spectrometer was utilized for recording ^{1}H NMR spectra at 400 MHz. The mass spectrum (in ESI mode) was measured with an Agilent 6520 Q-TOF high-resolution mass spectrometer.

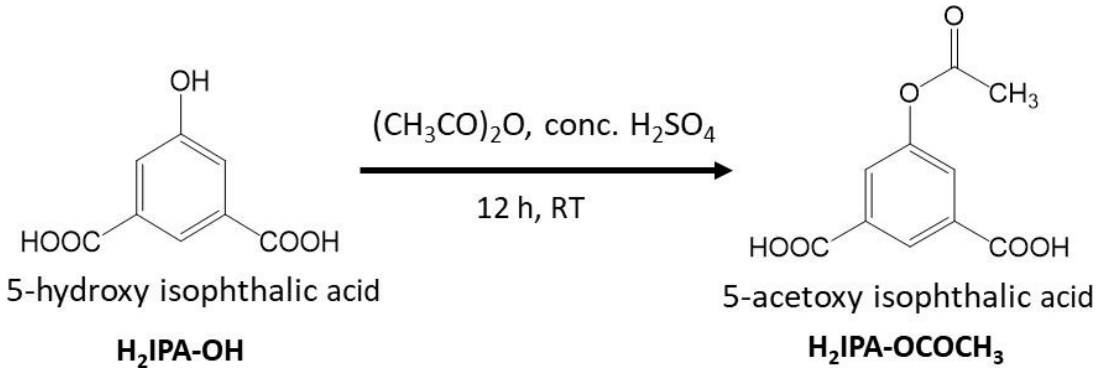

Scheme S1. Scheme for the preparation of 5-acetoxy isophthalic acid (H_2IPA-$OCOCH_3$) ligand.

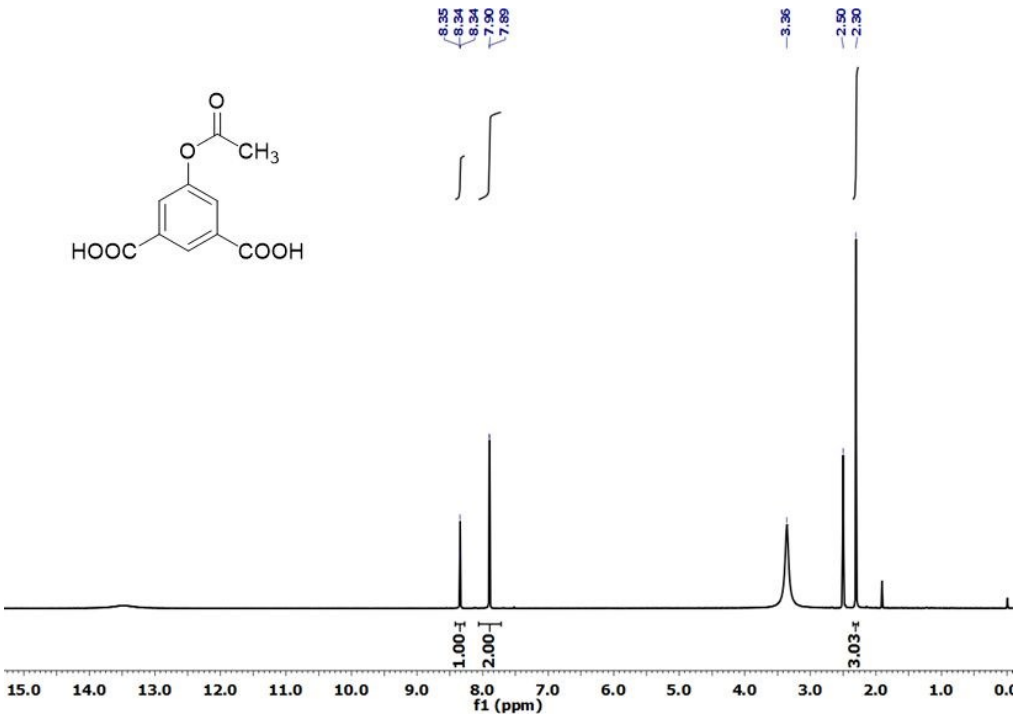

Figure S1. ^{1}H NMR spectrum of $H_2IPA\text{-}OCOCH_3$ ligand.

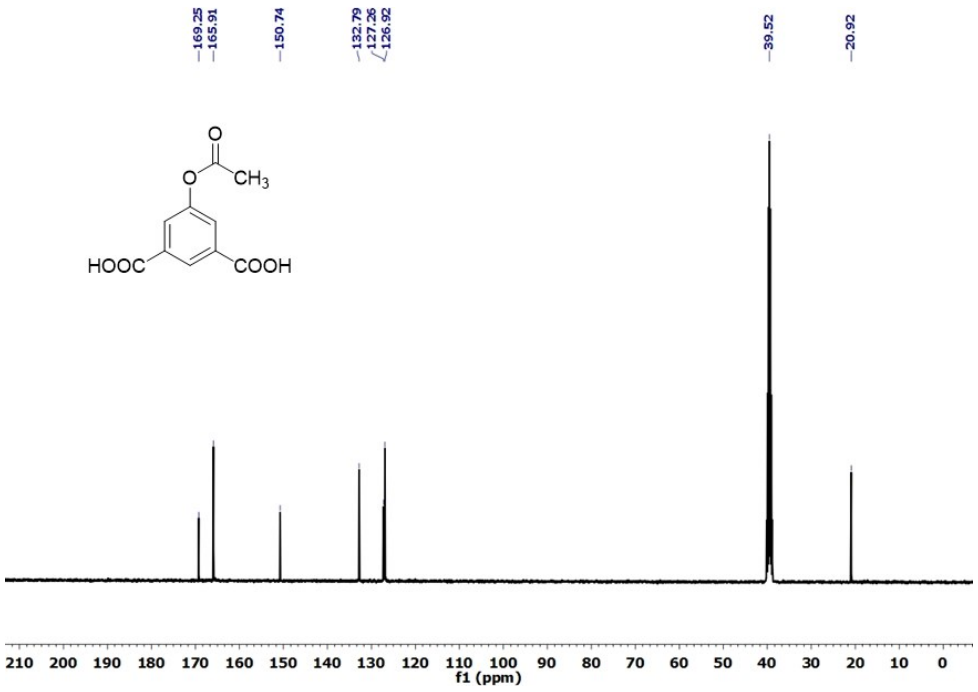

Figure S2. ^{13}C NMR spectrum of $H_2IPA\text{-}OCOCH_3$ ligand.

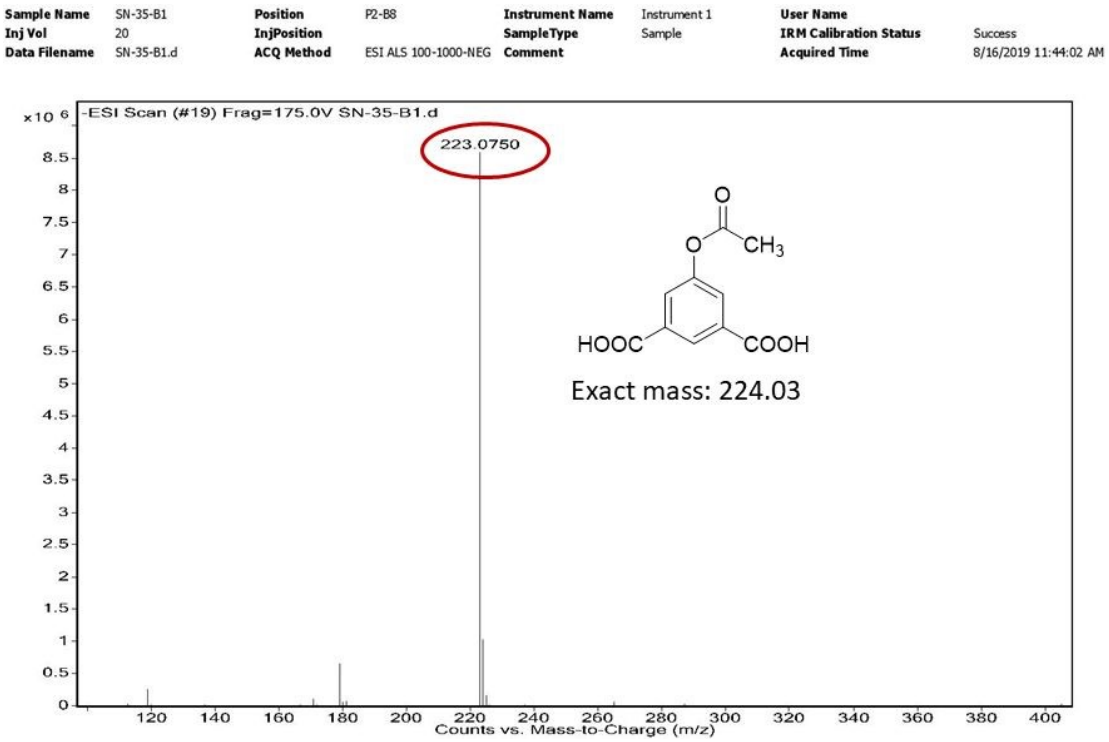

Figure S3. ESI-MS spectrum of H_2IPA-OCOCH$_3$ ligand.

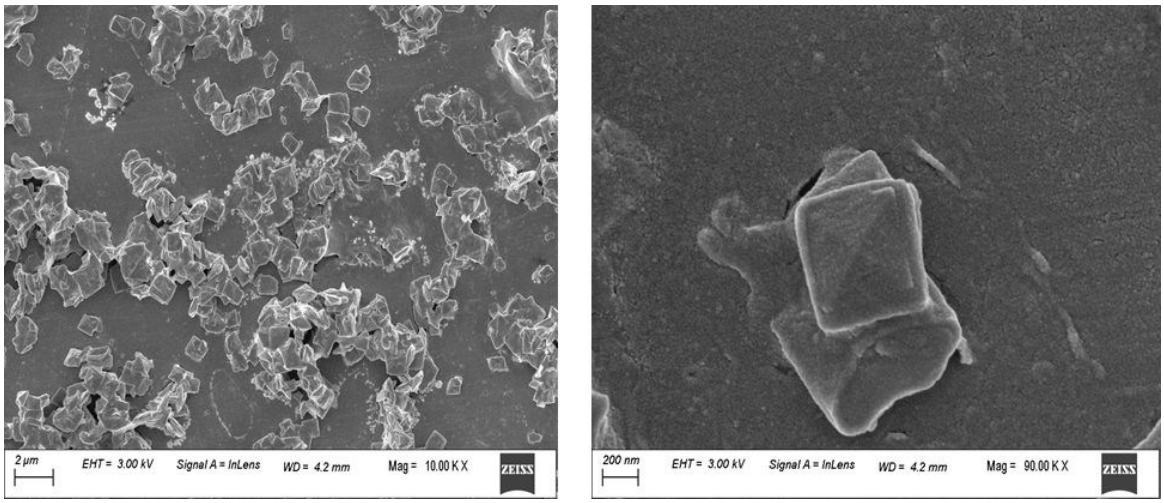

Figure S4. FE-SEM images of **1′** under different magnifications.

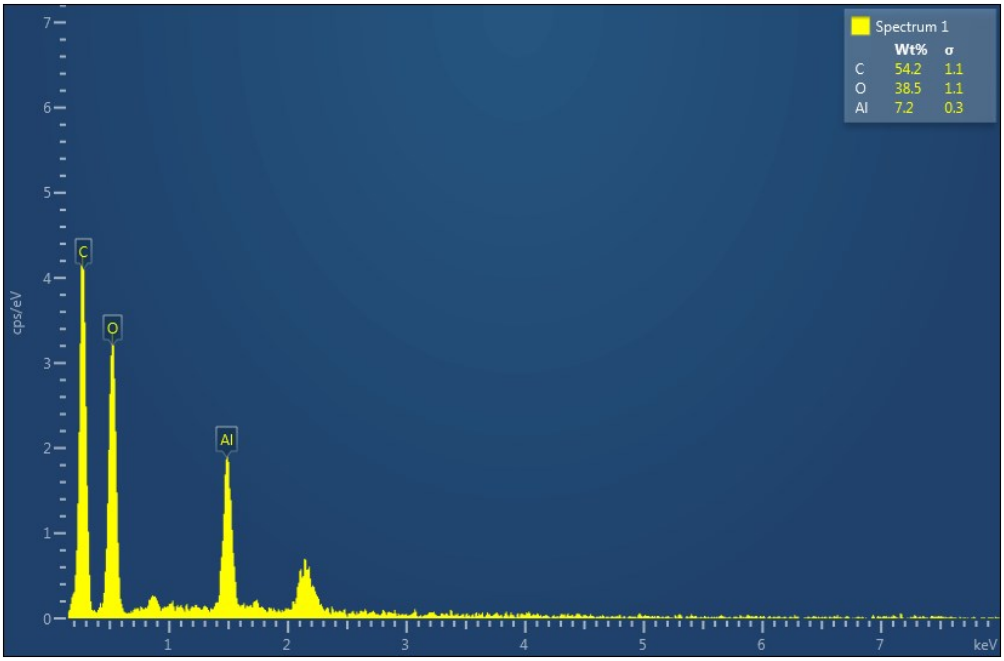

Figure S5. EDX spectrum of **1'**.

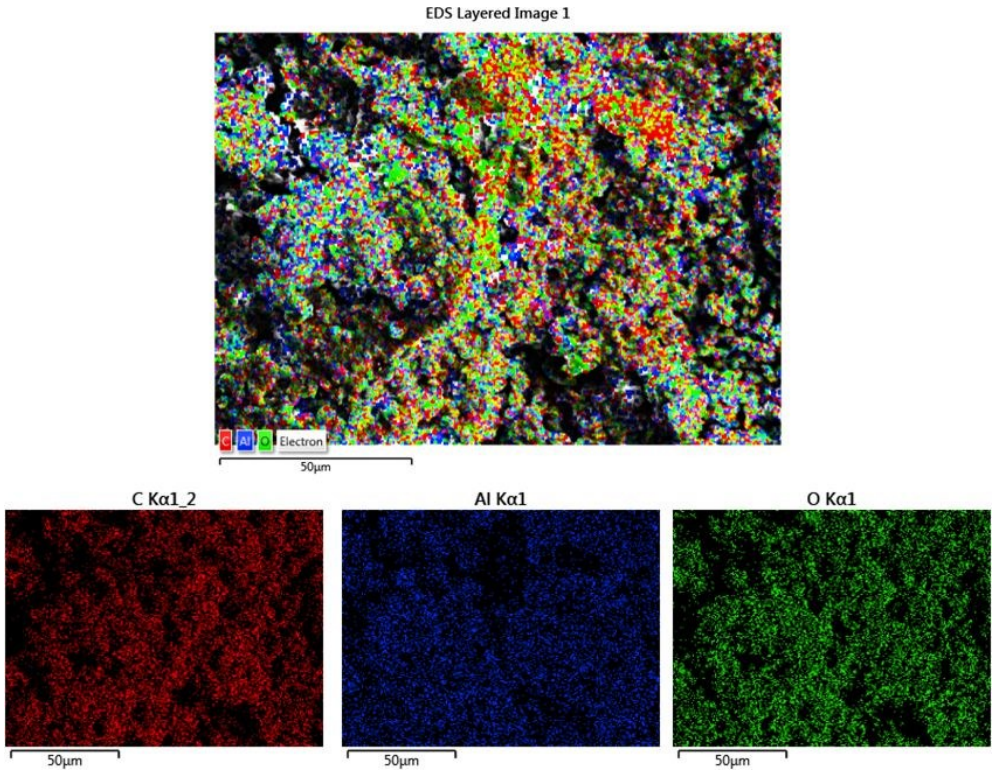

Figure S6. EDX elemental mapping of **1'**.

Table S1. Structural refinement parameters for **1**.

MOF	CAU-10-OCOCH$_3$
Crystal system	tetragonal
Space group	$I4_1md$
$a = b$ [Å]	21.3489(5)
c [Å]	10.9008(3)
$\alpha = \beta = \gamma$ [°]	90
R_{wp} [%]	3.8
GoF	1.9

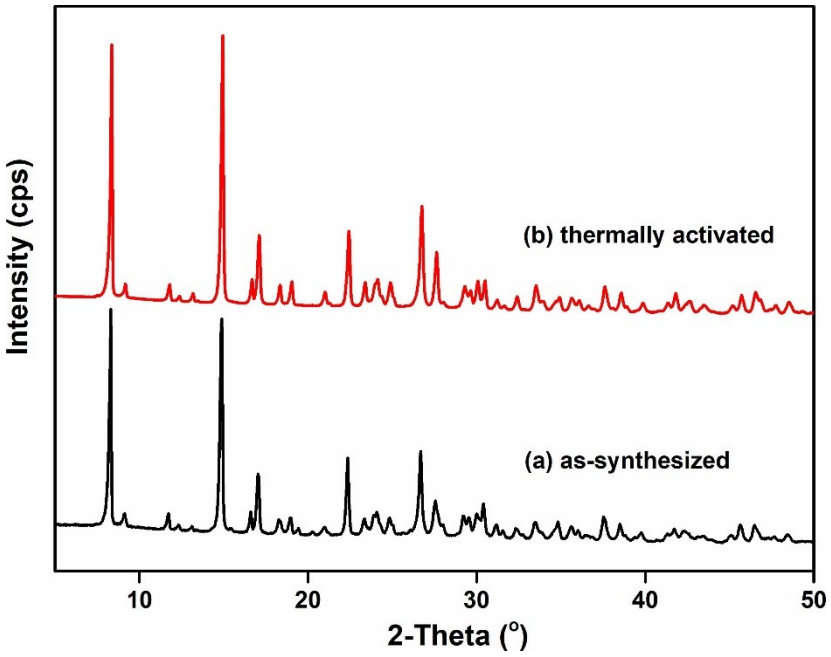

Figure S7. XRPD patterns of the as-synthesized (black) and activated (red) CAU-10-OCOCH$_3$ compound.

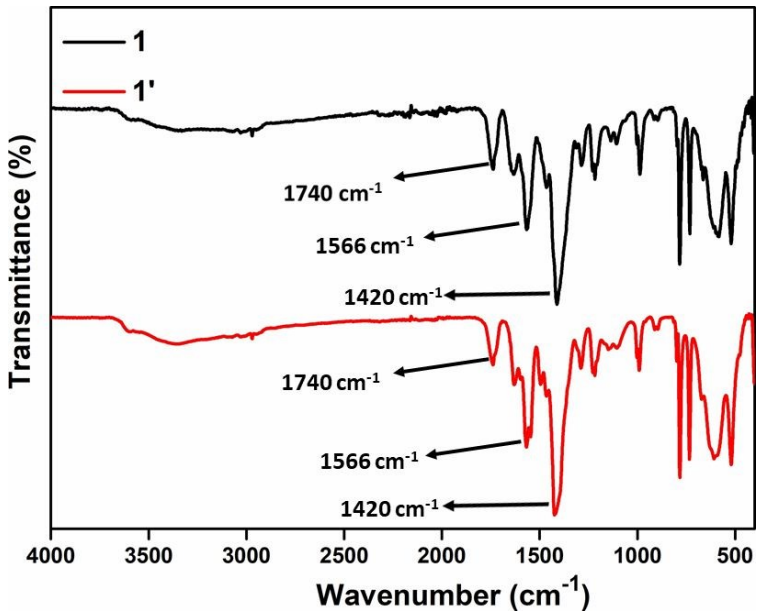

Figure S8. FT-IR spectra of as-synthesized **1** and thermally activated **1′**.

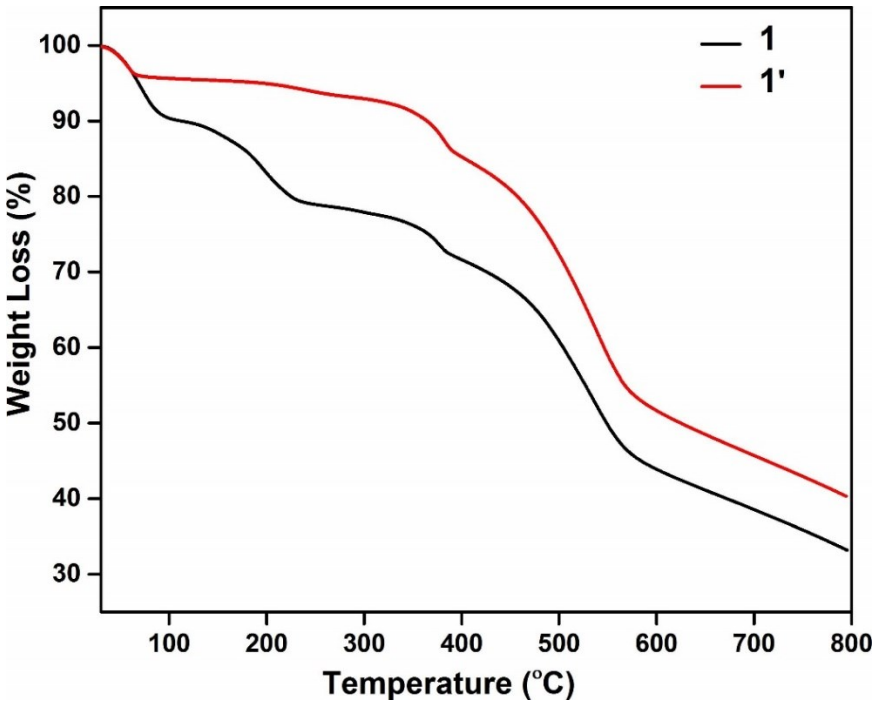

Figure S9. TG curves of as-synthesized and activated material measured in the temperature range of 25-800 °C at a heating rate of 10 ºC min^{-1}.

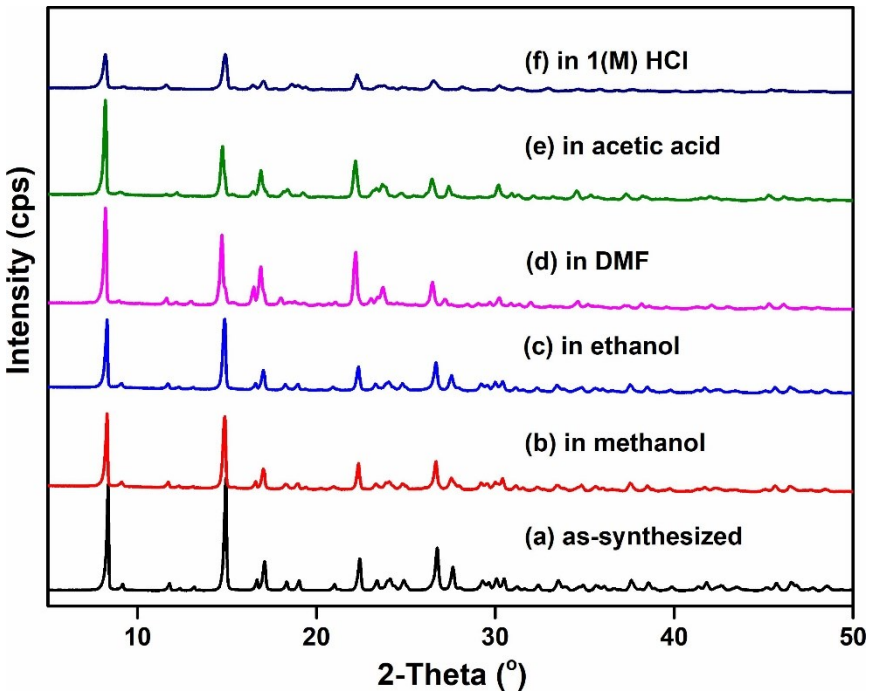

Figure S10. XRPD patterns of as-synthesized **1** (a), in methanol (b), in ethanol (c), in DMF (d), in acetic acid (e) and in 1 (M) HCl (i).

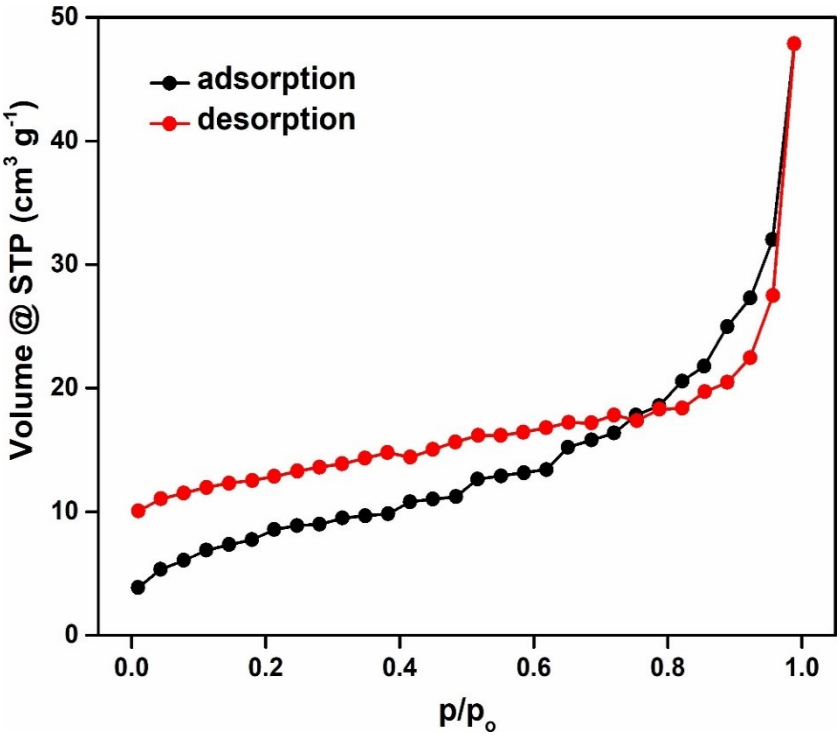

Figure S11. N_2 adsorption (solid black circles) and desorption (solid red circles) isotherms of activated compound measured at -196 °C.

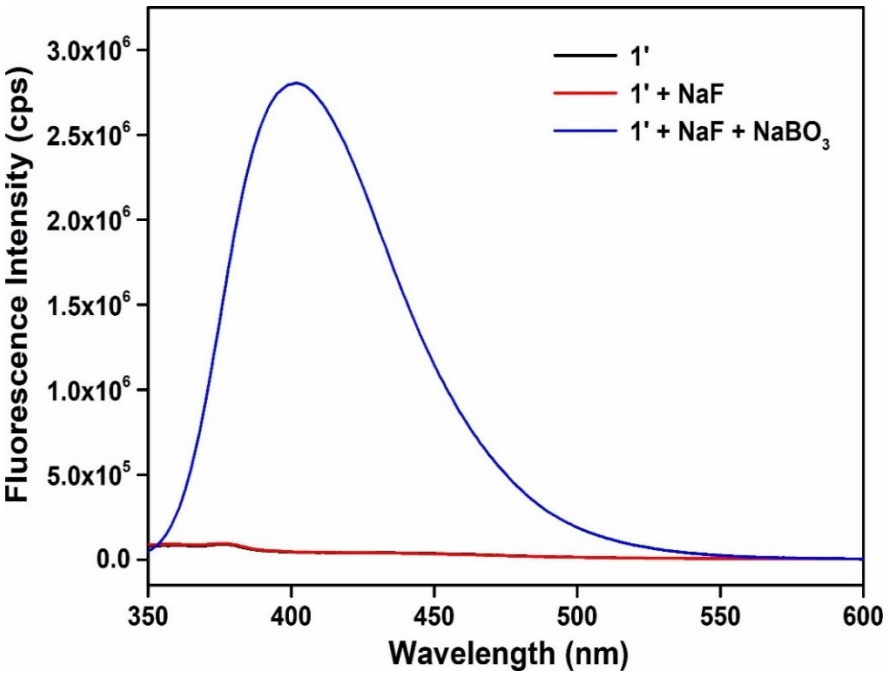

Figure S12. Change in the fluorescence emission intensity of **1′** upon addition of 10 mM $NaBO_3$ solution (500 µL) in presence of 10 mM NaF solution (500 µL).

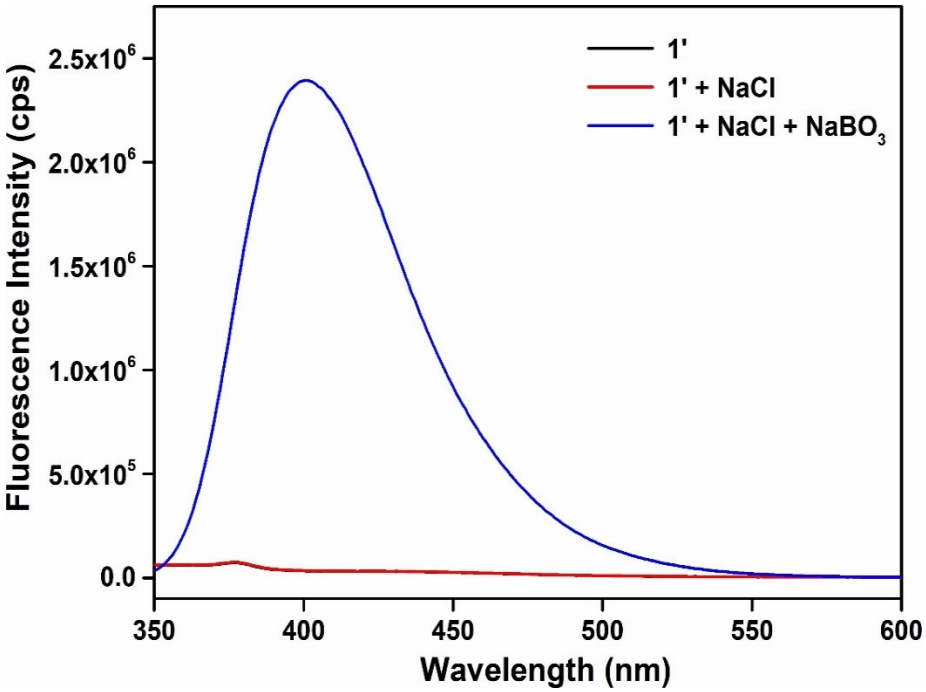

Figure S13. Change in the fluorescence emission intensity of **1′** upon addition of 10 mM $NaBO_3$ solution (500 µL) in presence of 10 mM NaCl solution (500 µL).

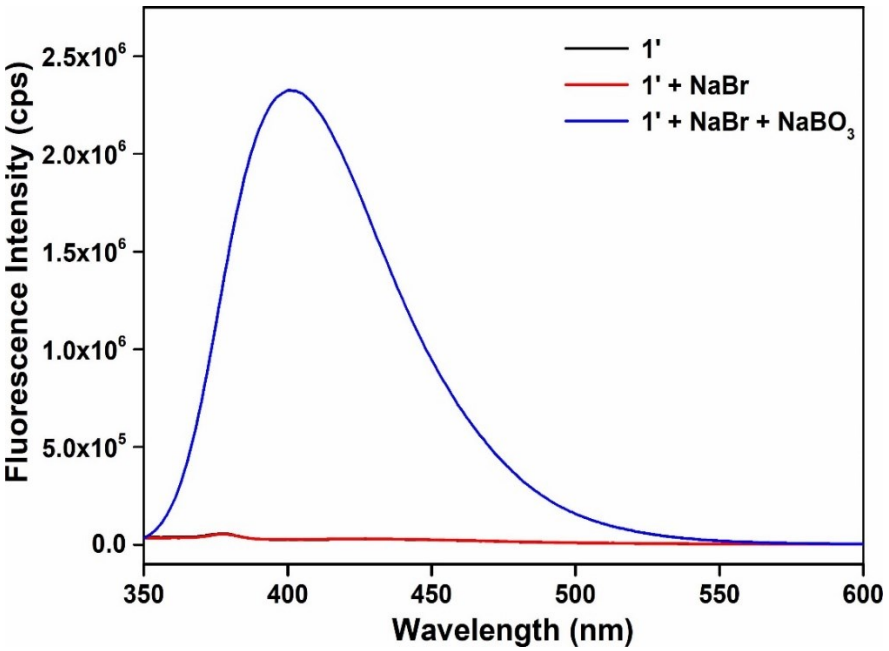

Figure S14. Change in the fluorescence emission intensity of **1′** upon addition of 10 mM $NaBO_3$ solution (500 µL) in presence of 10 mM NaBr solution (500 µL).

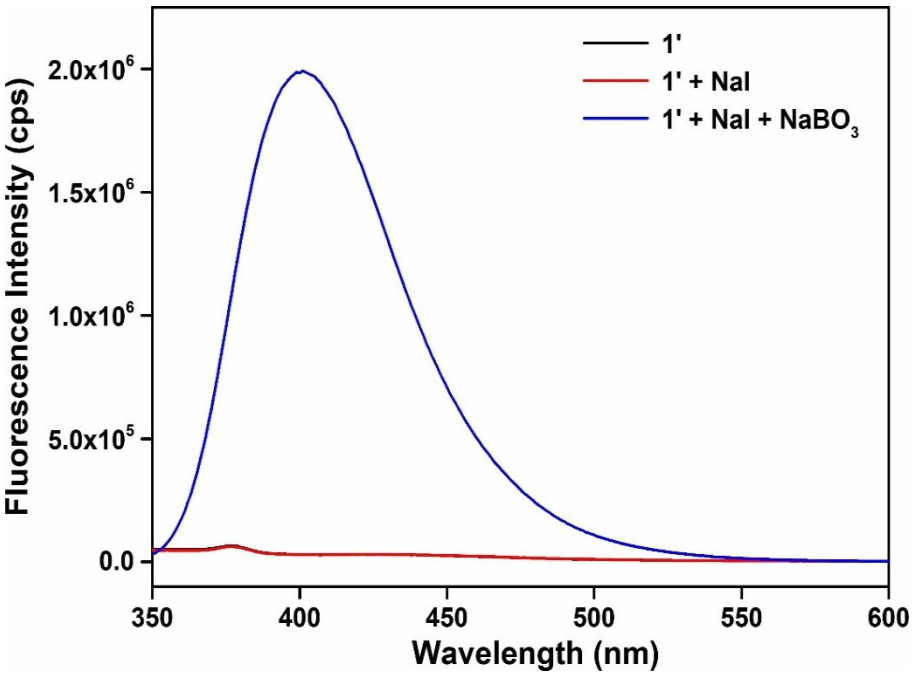

Figure S15. Change in the fluorescence emission intensity of **1′** upon addition of 10 mM $NaBO_3$ solution (500 µL) in presence of 10 mM NaI solution (500 µL).

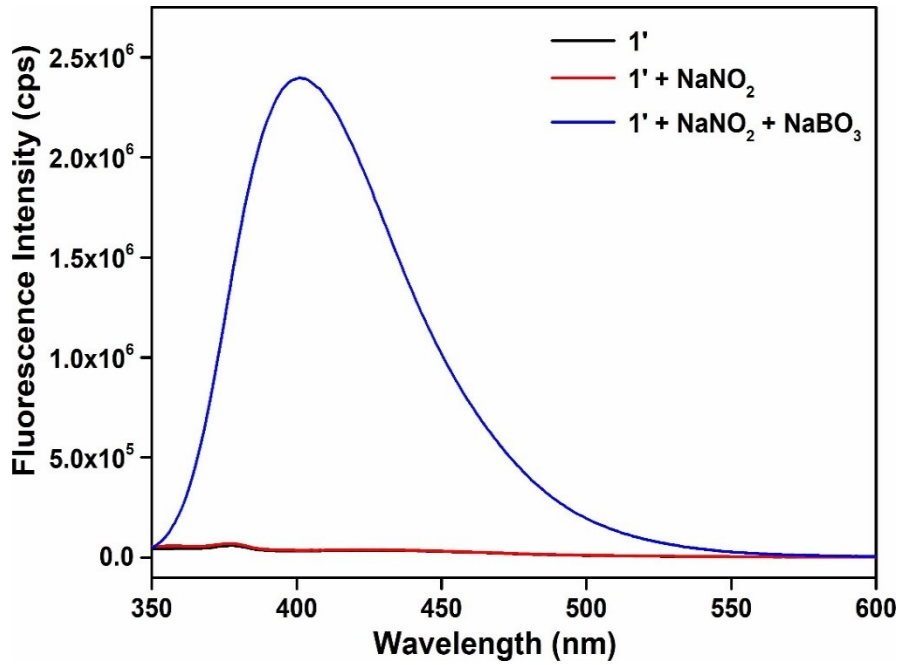

Figure S16. Change in the fluorescence emission intensity of **1′** upon addition of 10 mM $NaBO_3$ solution (500 µL) in presence of 10 mM $NaNO_2$ solution (500 µL).

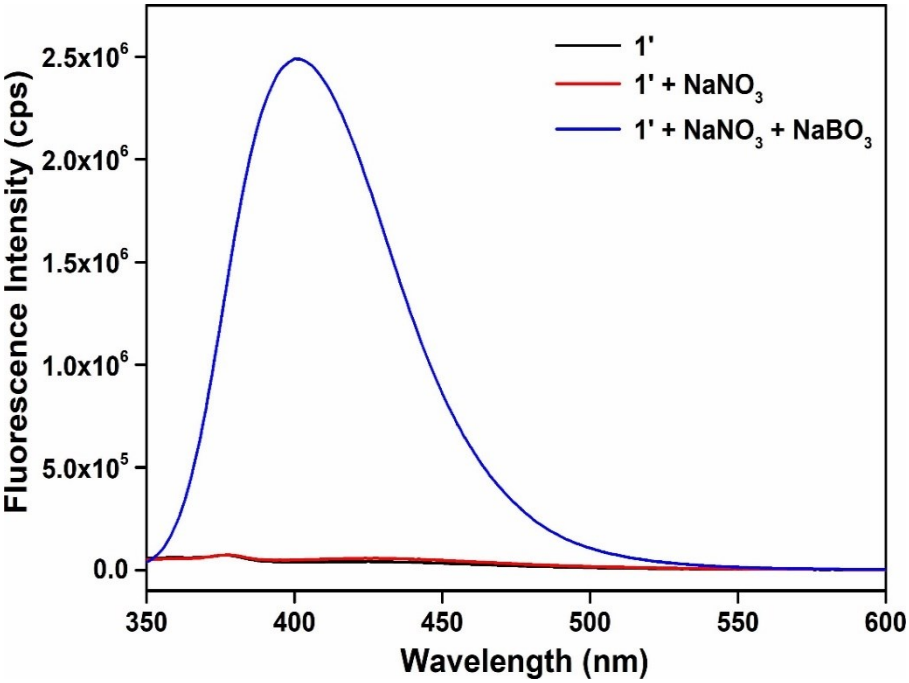

Figure S17. Change in the fluorescence emission intensity of **1′** upon addition of 10 mM $NaBO_3$ solution (500 µL) in presence of 10 mM $NaNO_3$ solution (500 µL).

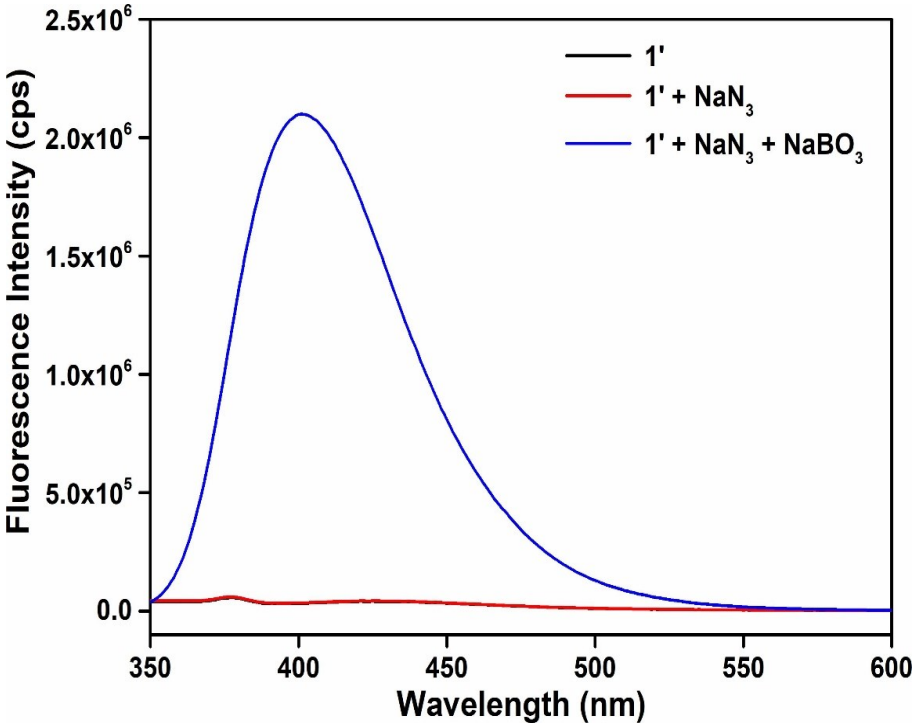

Figure S18. Change in the fluorescence emission intensity of **1′** upon addition of 10 mM $NaBO_3$ solution (500 µL) in presence of 10 mM NaN_3 solution (500 µL).

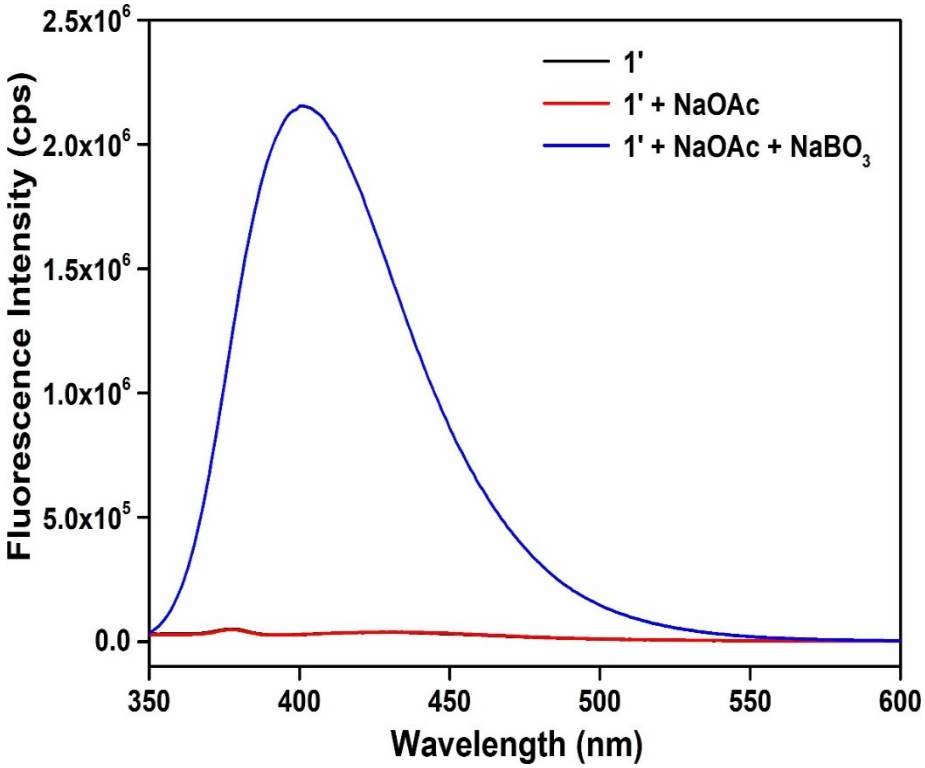

Figure S19. Change in the fluorescence emission intensity of **1′** upon addition of 10 mM $NaBO_3$ solution (500 µL) in presence of 10 mM NaOAc solution (500 µL).

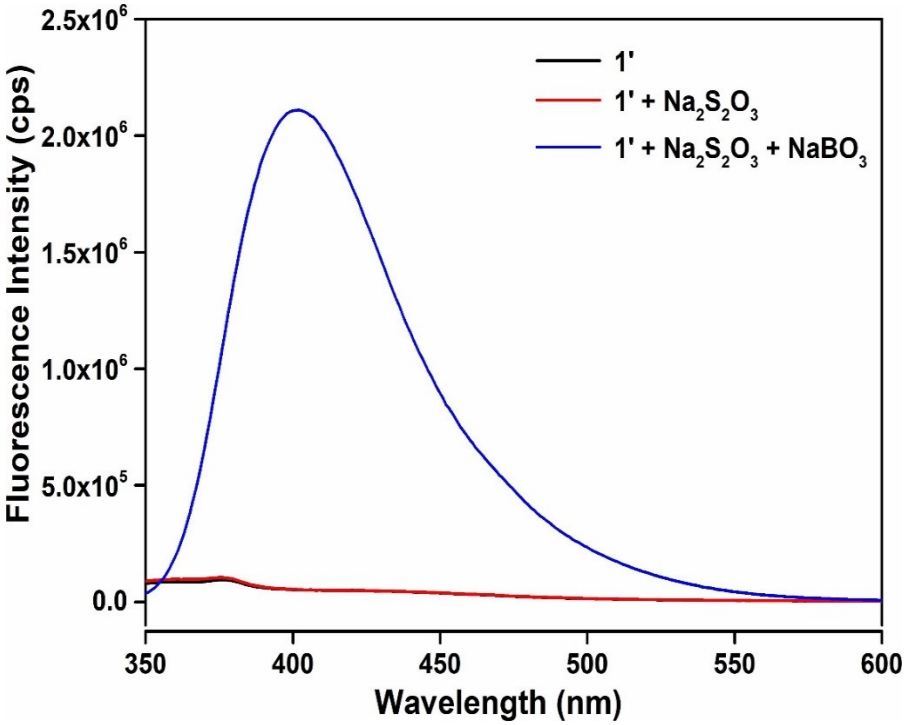

Figure S20. Change in the fluorescence emission intensity of **1′** upon addition of 10 mM $NaBO_3$ solution (500 µL) in presence of 10 mM $Na_2S_2O_3$ solution (500 µL).

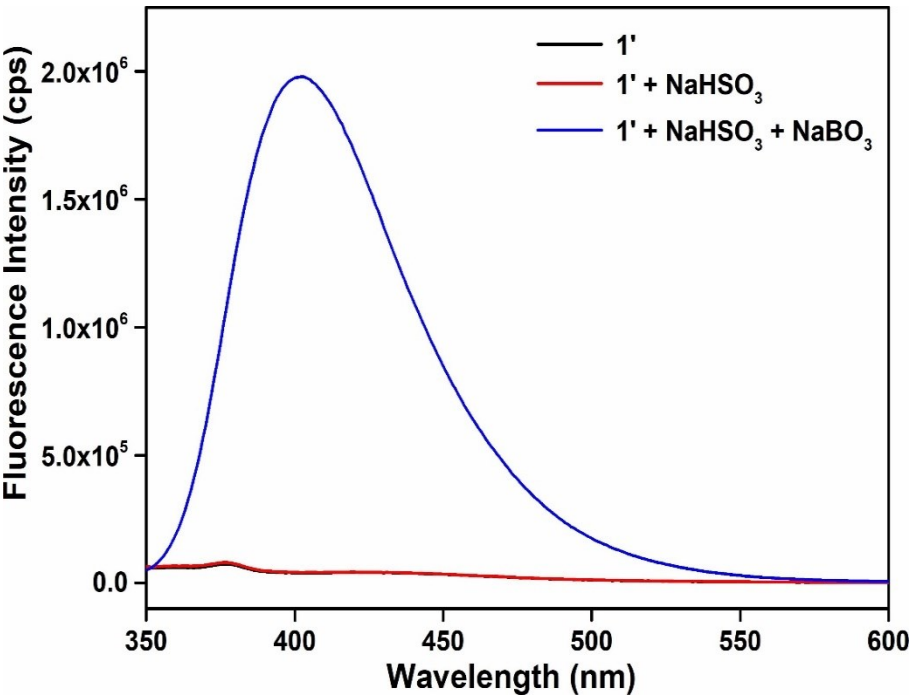

Figure S21. Change in the fluorescence emission intensity of **1′** upon addition of 10 mM $NaBO_3$ solution (500 µL) in presence of 10 mM $NaHSO_3$ solution (500 µL).

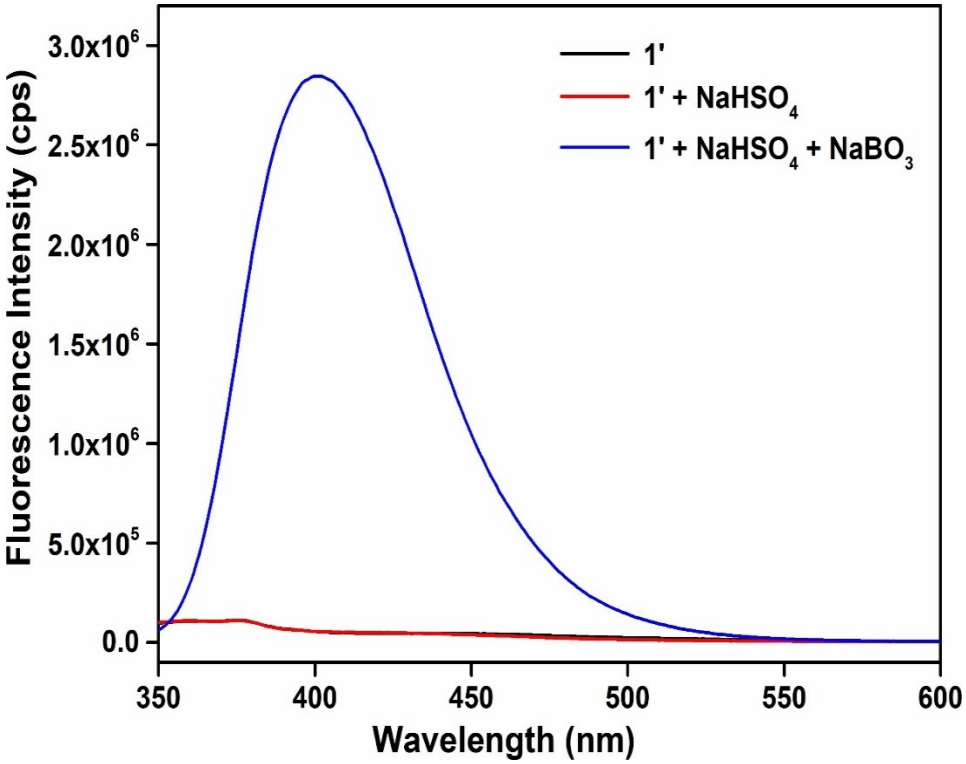

Figure S22. Change in the fluorescence emission intensity of **1′** upon addition of 10 mM $NaBO_3$ solution (500 µL) in presence of 10 mM $NaHSO_4$ solution (500 µL).

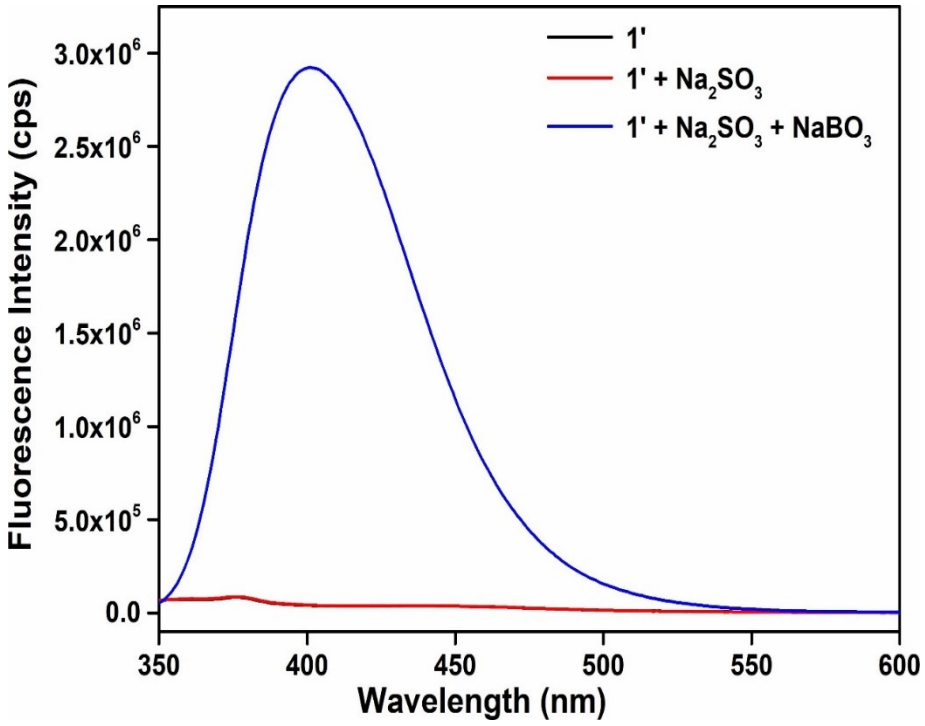

Figure S23. Change in the fluorescence emission intensity of **1′** upon addition of 10 mM $NaBO_3$ solution (500 µL) in presence of 10 mM Na_2SO_3 solution (500 µL).

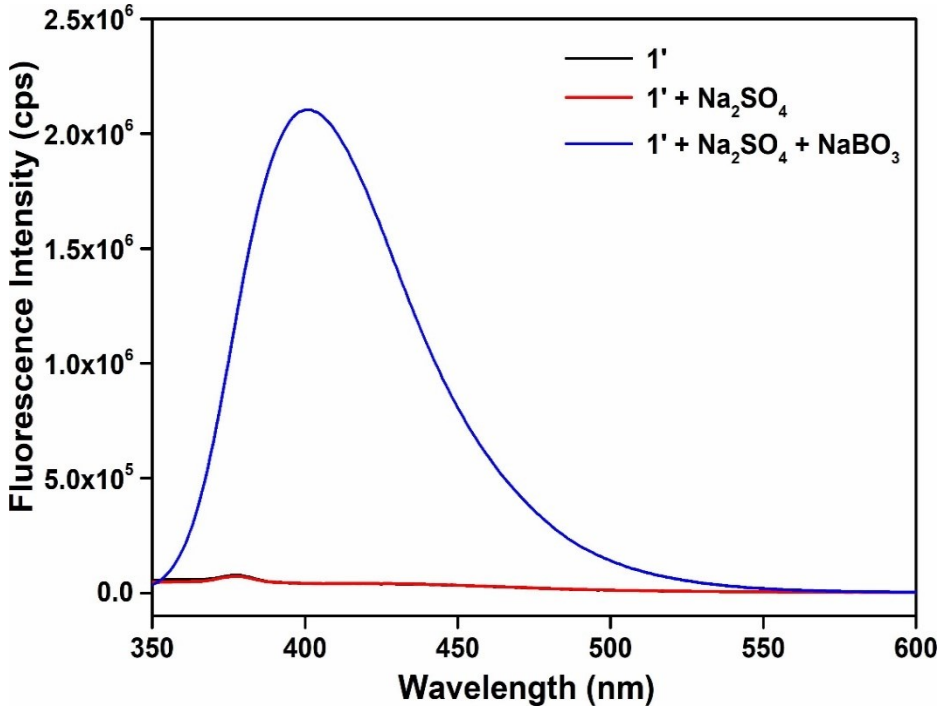

Figure S24. Change in the fluorescence emission intensity of **1′** upon addition of 10 mM $NaBO_3$ solution (500 µL) in presence of 10 mM Na_2SO_4 solution (500 µL).

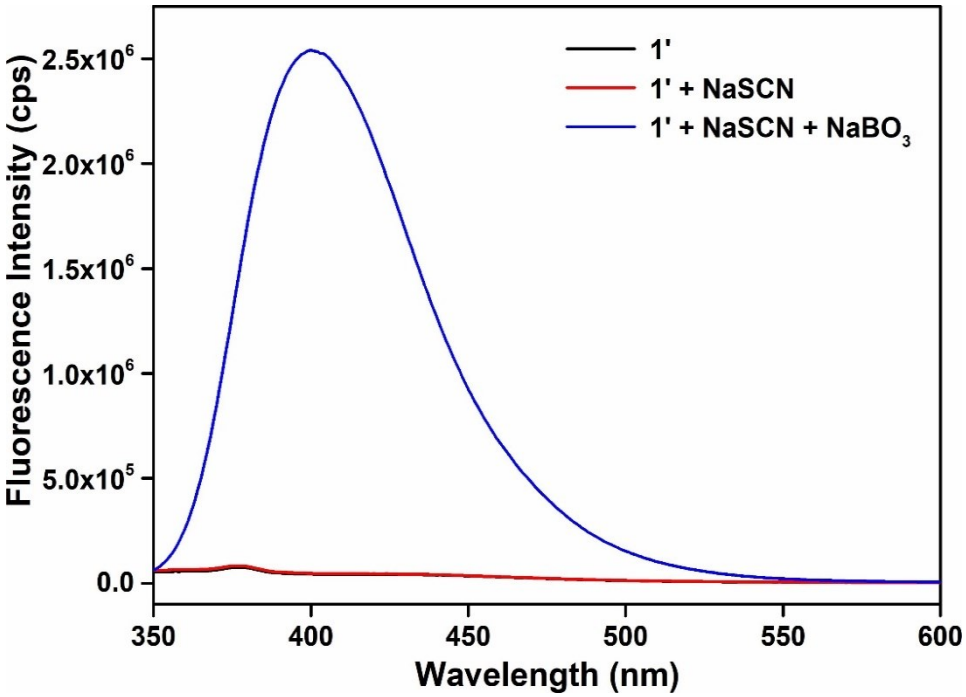

Figure S25. Change in the fluorescence emission intensity of **1′** upon addition of 10 mM $NaBO_3$ solution (500 µL) in presence of 10 mM NaSCN solution (500 µL).

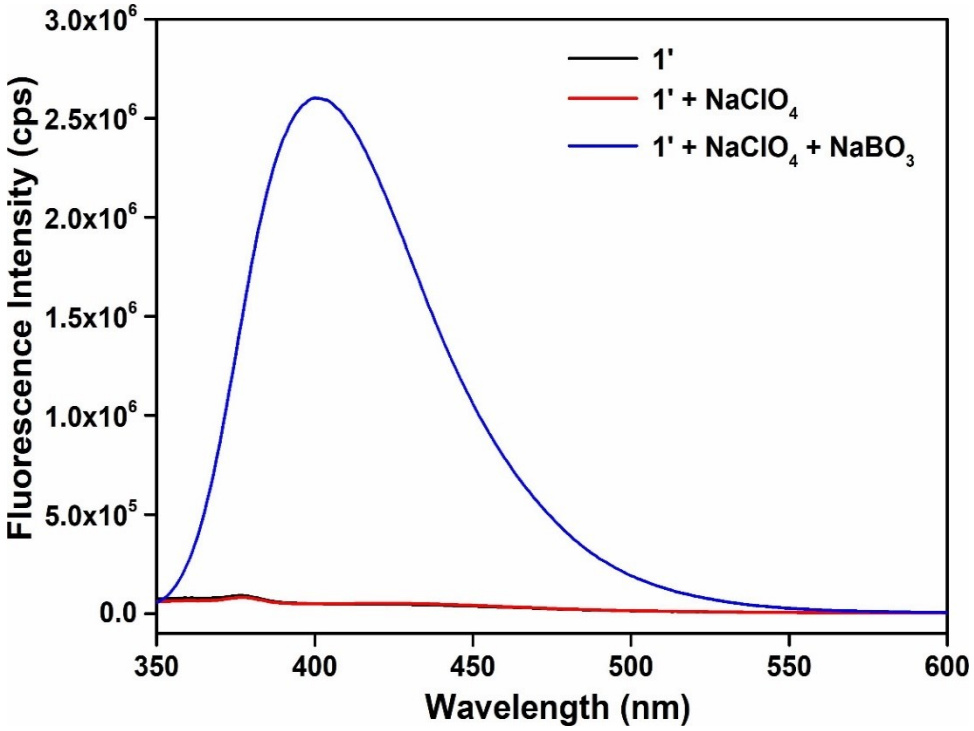

Figure S26. Change in the fluorescence emission intensity of **1′** upon addition of 10 mM $NaBO_3$ solution (500 µL) in presence of 10 mM $NaClO_4$ solution (500 µL).

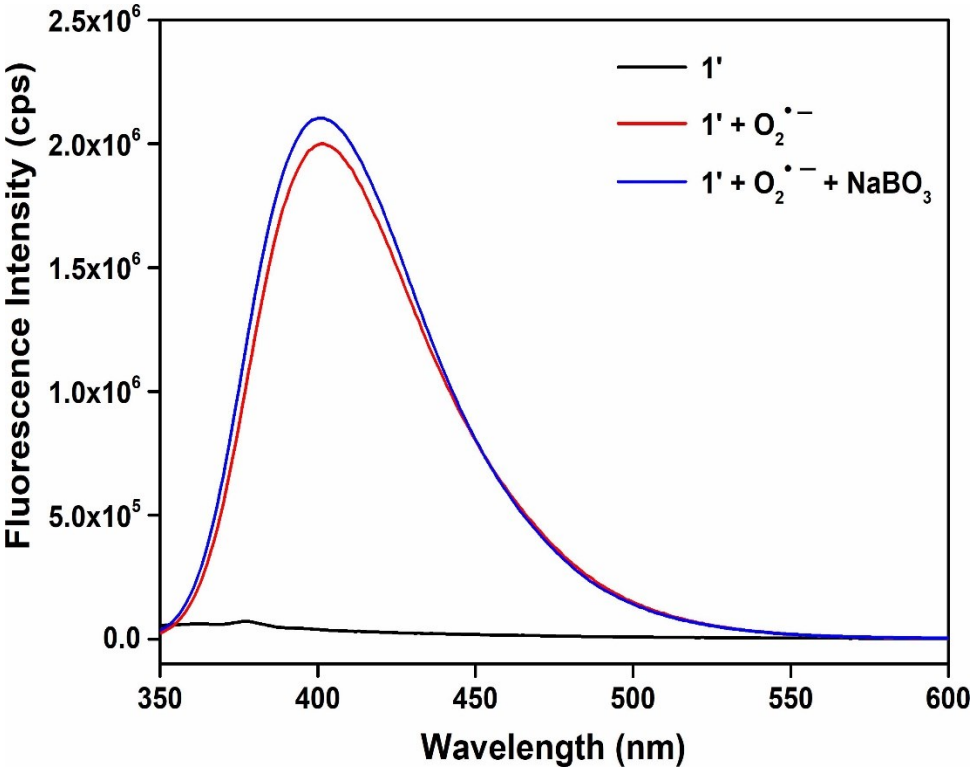

Figure S27. Change in the fluorescence emission intensity of **1′** upon addition of 10 mM $NaBO_3$ solution (500 µL) in presence of 10 mM $O_2^{\bullet-}$solution (500 µL).

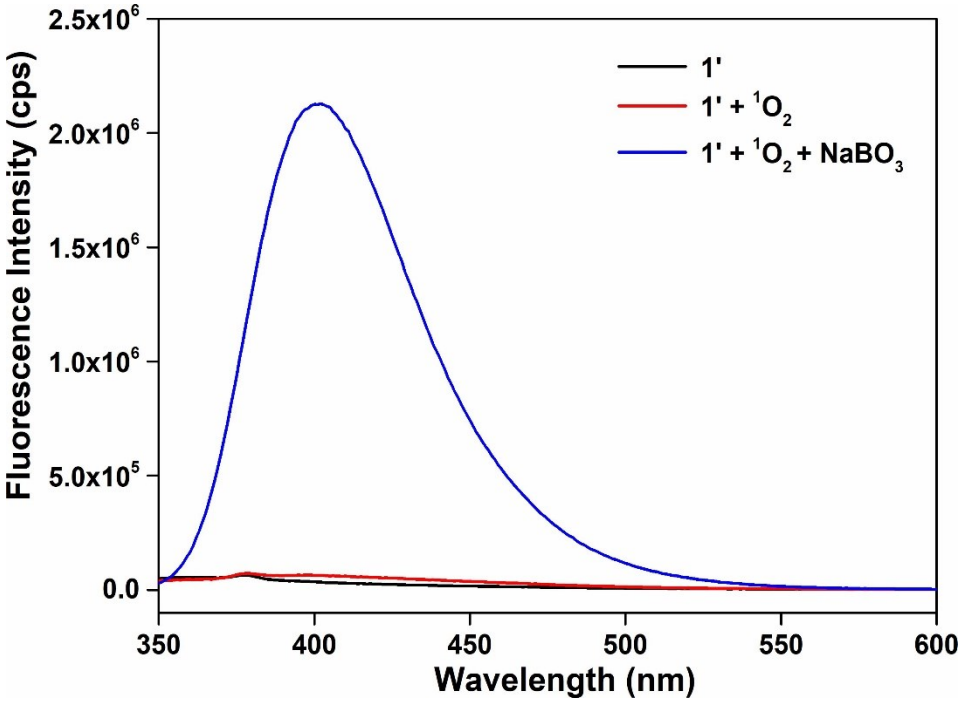

Figure S28. Change in the fluorescence emission intensity of **1′** upon addition of 10 mM $NaBO_3$ solution (500 µL) in presence of 10 mM $^1O_2$ solution (500 µL).

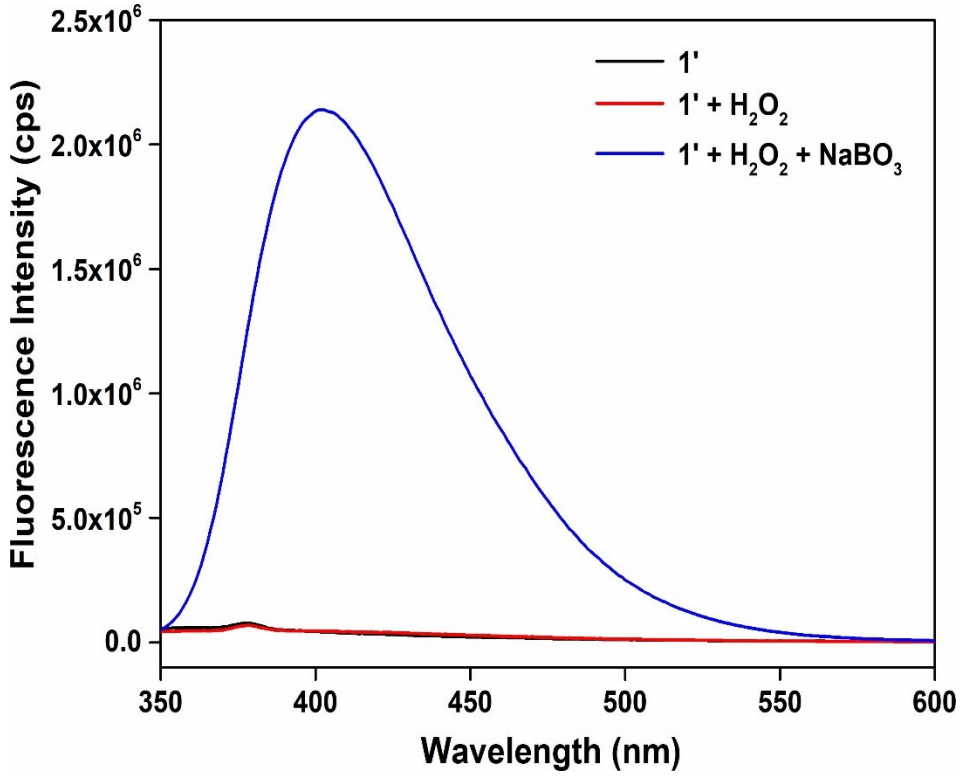

Figure S29. Change in the fluorescence emission intensity of **1′** upon addition of 10 mM $NaBO_3$ solution (500 µL) in presence of 10 mM H_2O_2 solution (500 µL).

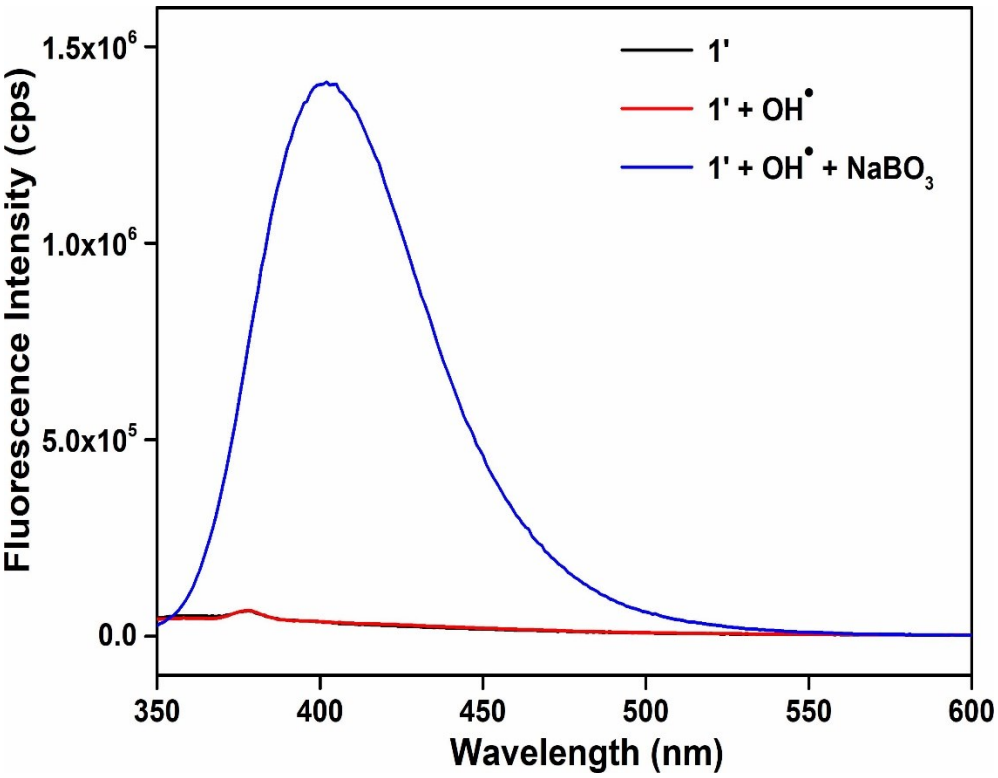

Figure S30. Change in the fluorescence emission intensity of **1′** upon addition of 10 mM $NaBO_3$ solution (500 µL) in presence of 10 mM OH• solution (500 µL).

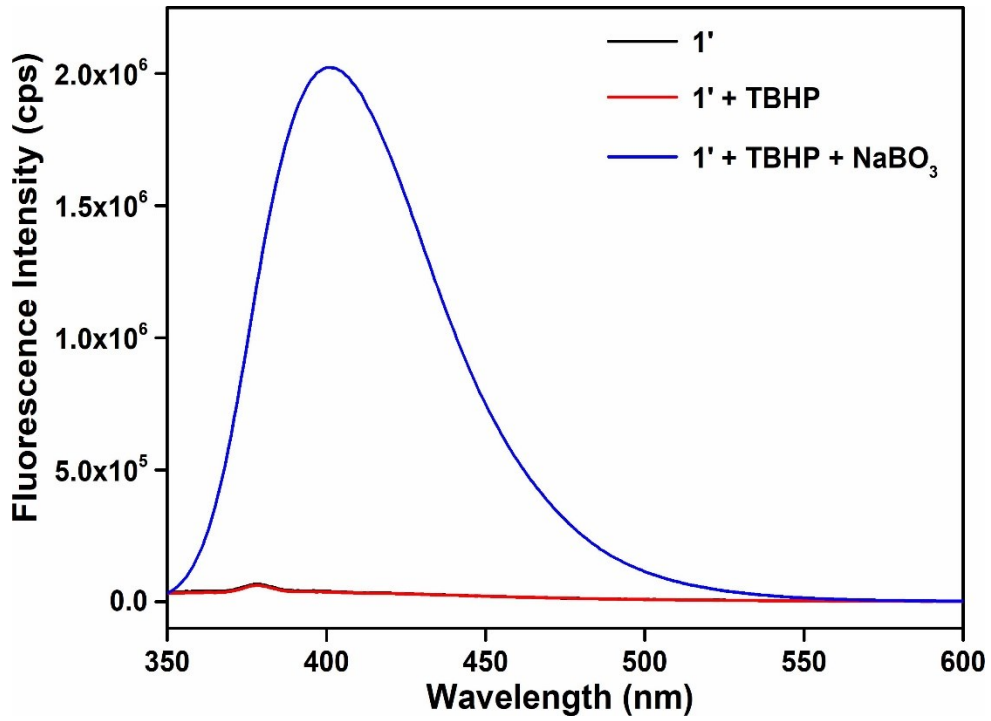

Figure S31. Change in the fluorescence emission intensity of **1′** upon addition of 10 mM $NaBO_3$ solution (500 µL) in presence of 10 mM TBHP solution (500 µL).

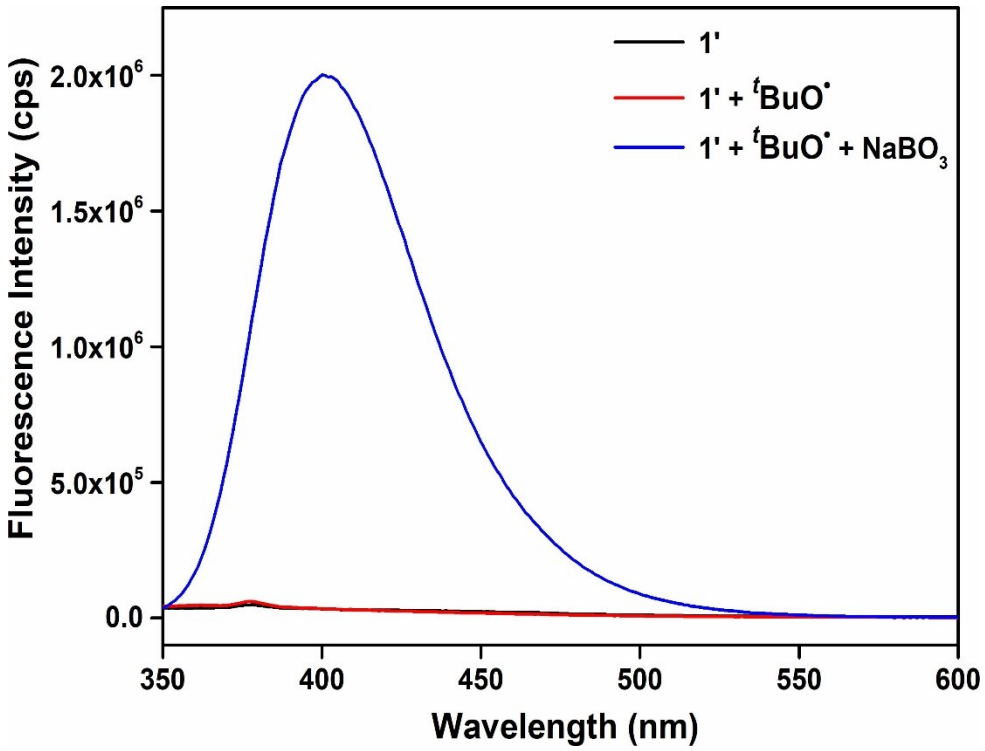

Figure S32. Change in the fluorescence emission intensity of **1′** upon addition of 10 mM $NaBO_3$ solution (500 µL) in presence of 10 mM $^tBuO^\bullet$ solution (500 µL).

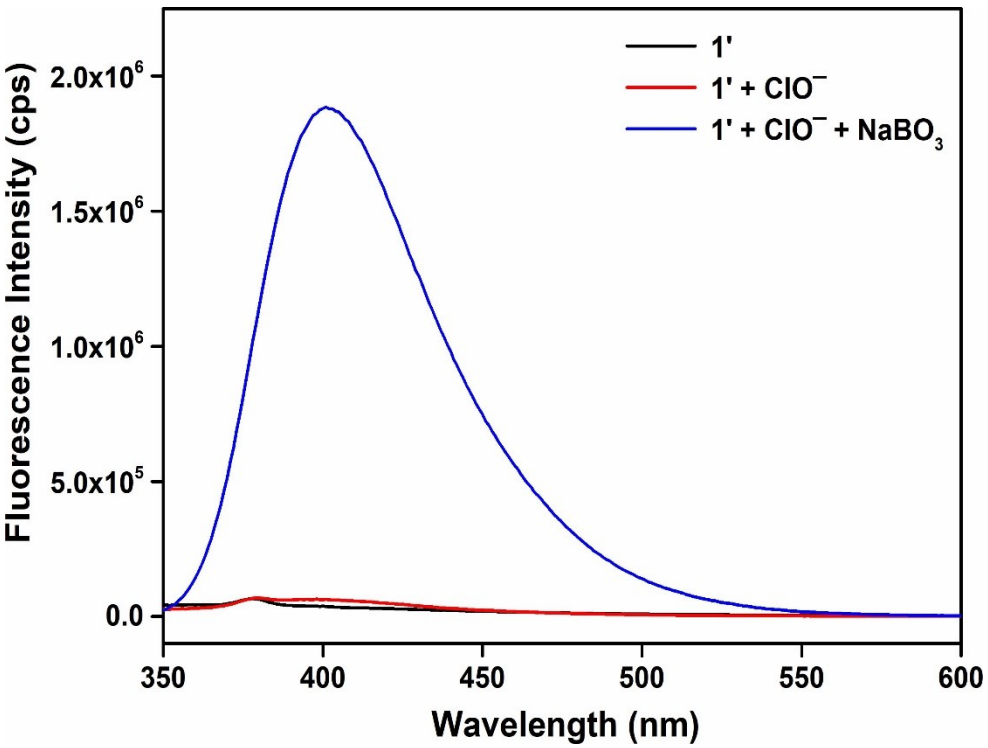

Figure S33. Change in the fluorescence emission intensity of **1′** upon addition of 10 mM $NaBO_3$ solution (500 µL) in presence of 10 mM ClO^- solution (500 µL).

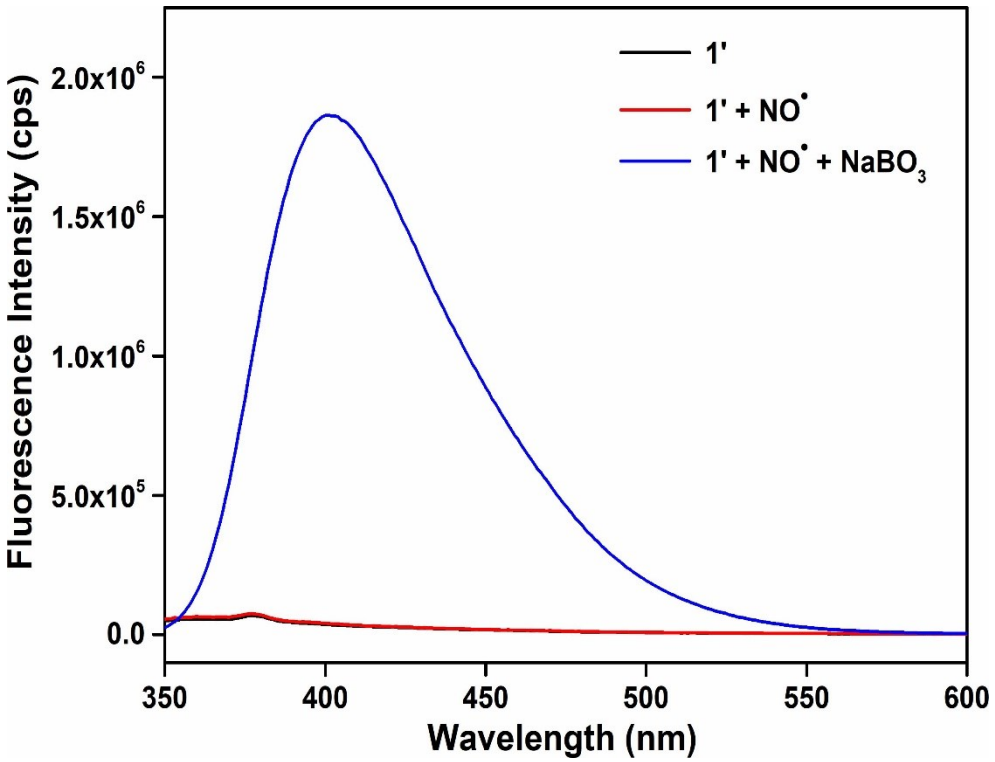

Figure S34. Change in the fluorescence emission intensity of **1′** upon addition of 10 mM $NaBO_3$ solution (500 µL) in presence of 10 mM $NO^{\bullet}$ solution (500 µL).

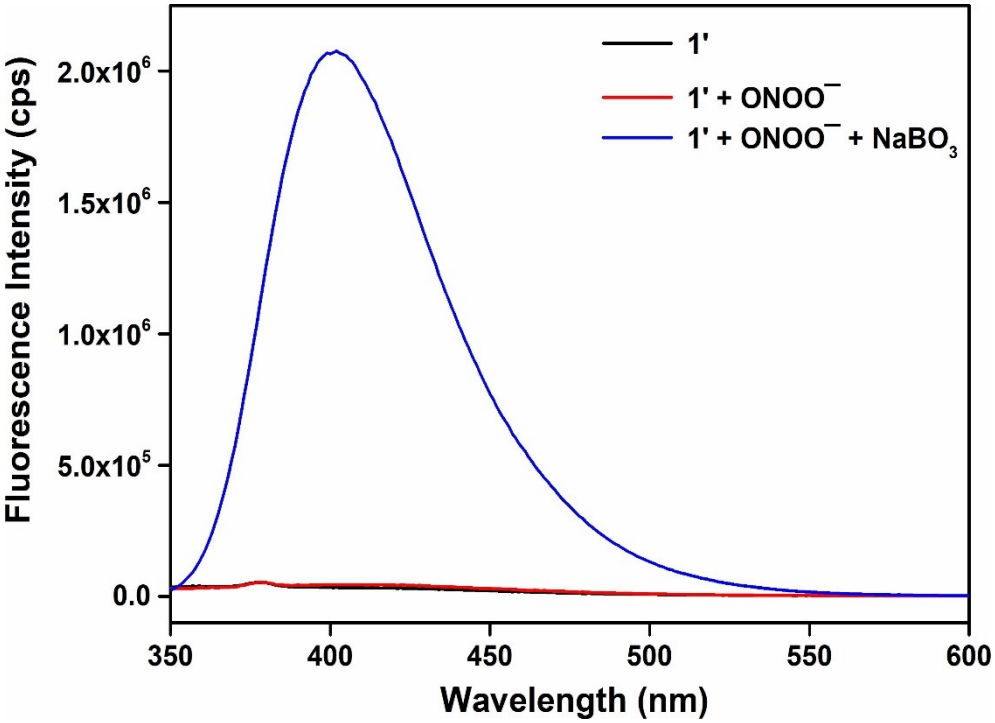

Figure S35. Change in the fluorescence emission intensity of **1′** upon addition of 10 mM $NaBO_3$ solution (500 µL) in presence of 10 mM $ONOO^{-}$ solution (500 µL).

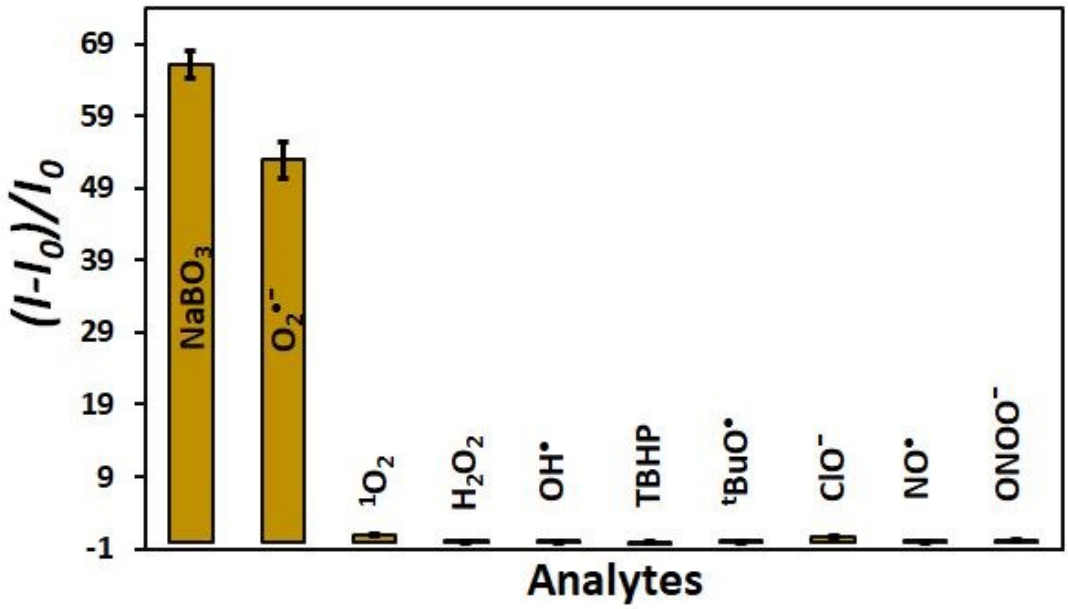

Figure S36. Fluorescence enhancement effect of **1′** towards the introduction of different ROS and RNS (10 mM, 500 µL) in aqueous medium. The error bars indicate the standard deviations of three measurements.

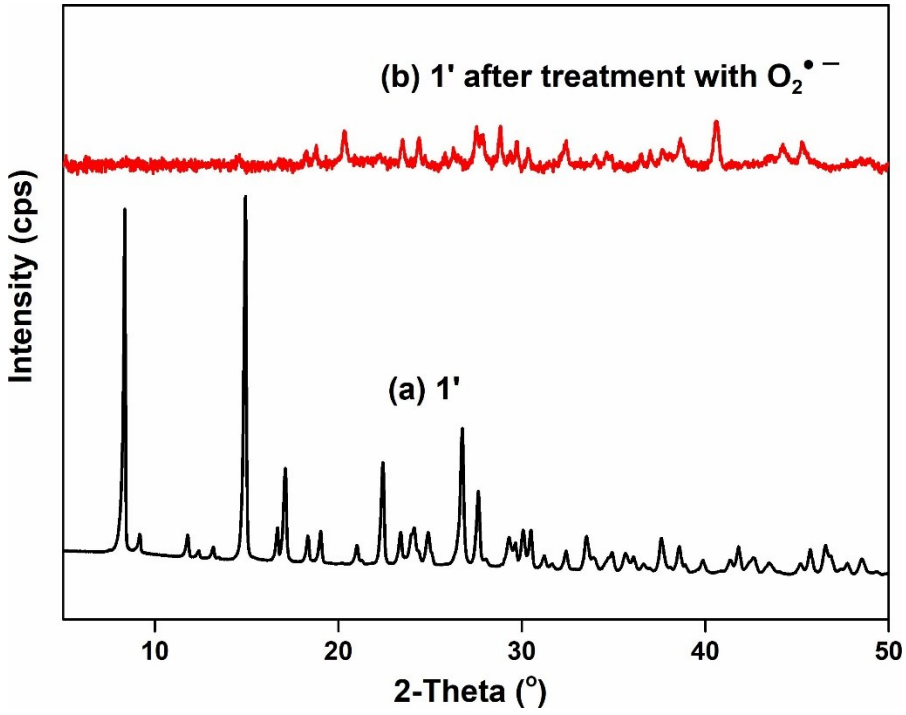

Figure S37. XRPD patterns of thermally activated (**1′**) (a) and after treatment with superoxide (b).

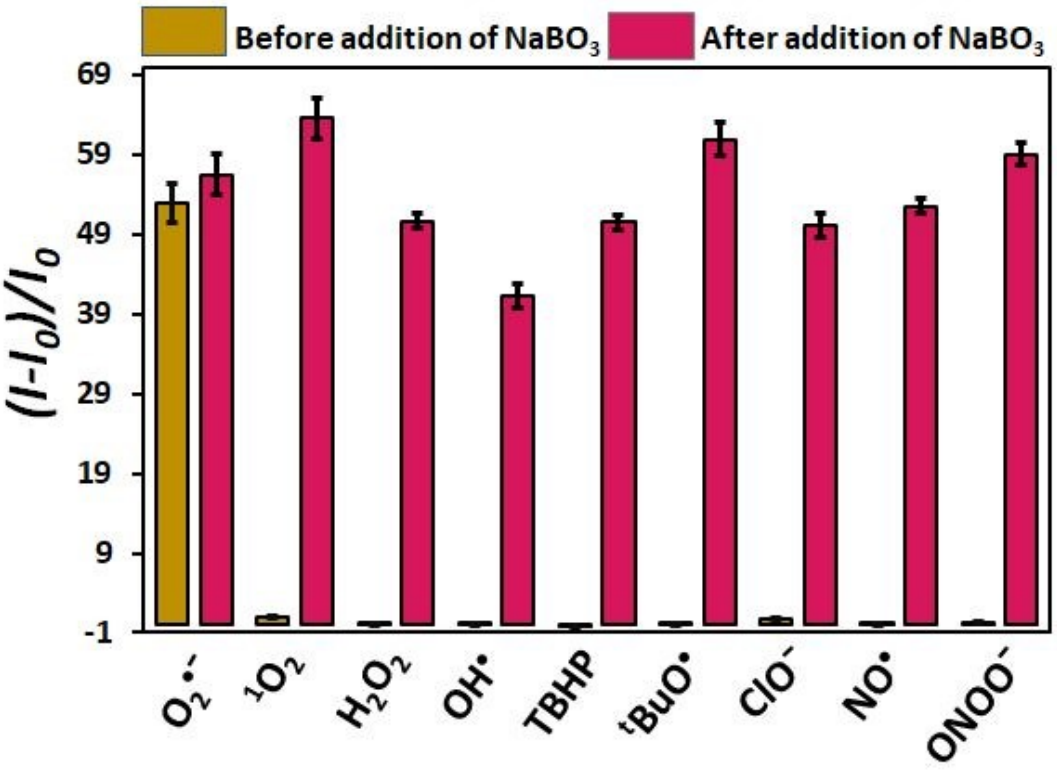

Figure S38. Effect in the emission intensity of aqueous suspension of **1′** by the addition of perborate solution (10 mM, 500 μL) in the co-existence of ROS and RNS. The error bars indicate the standard deviations of three measurements.

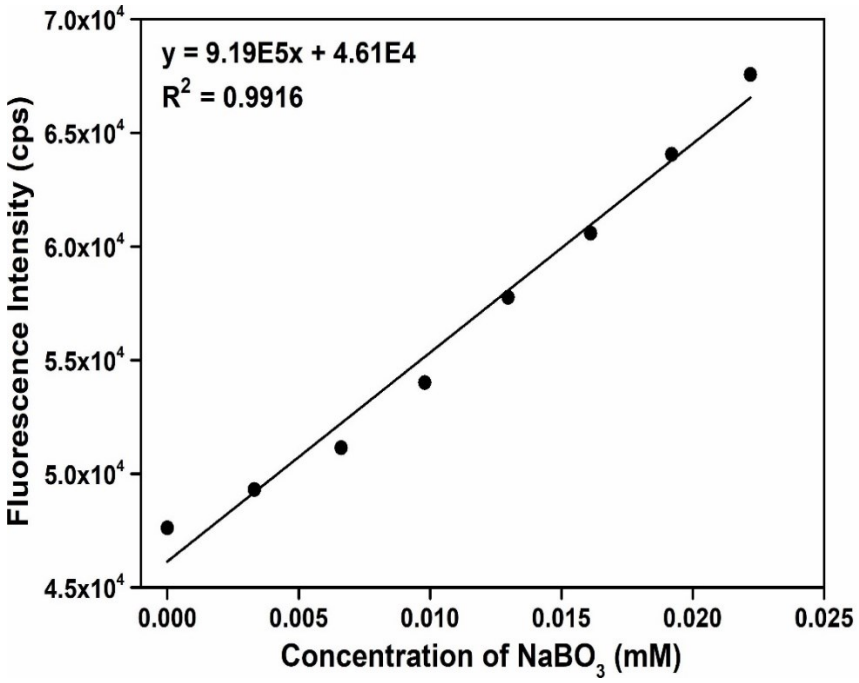

Figure S39. Change in the fluorescence emission intensity of **1′** in aqueous medium as a function of $NaBO_3$ concentration.

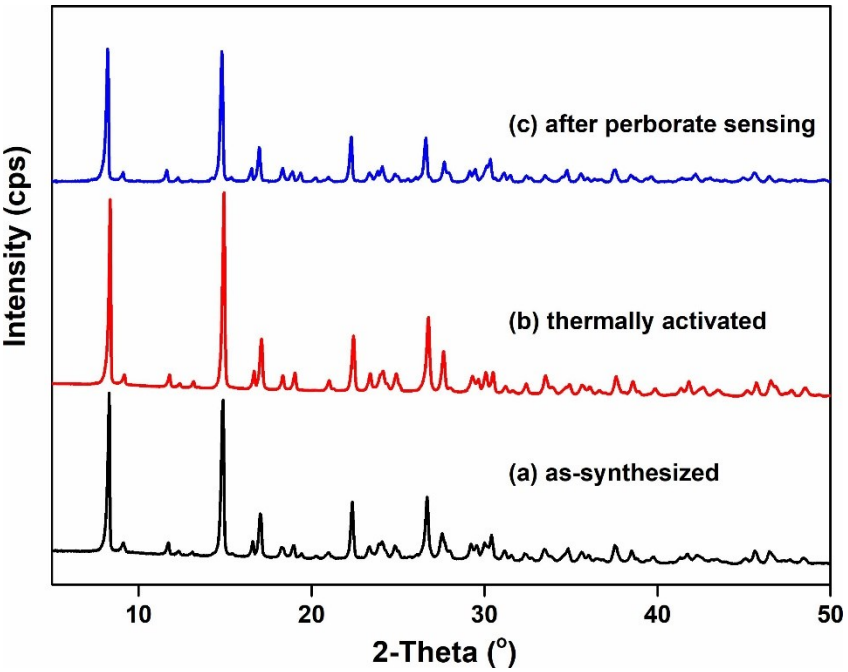

Figure S40. XRPD patterns of **1** in different forms: as-synthesized (a), thermally activated (b) and after perborate sensing (c).

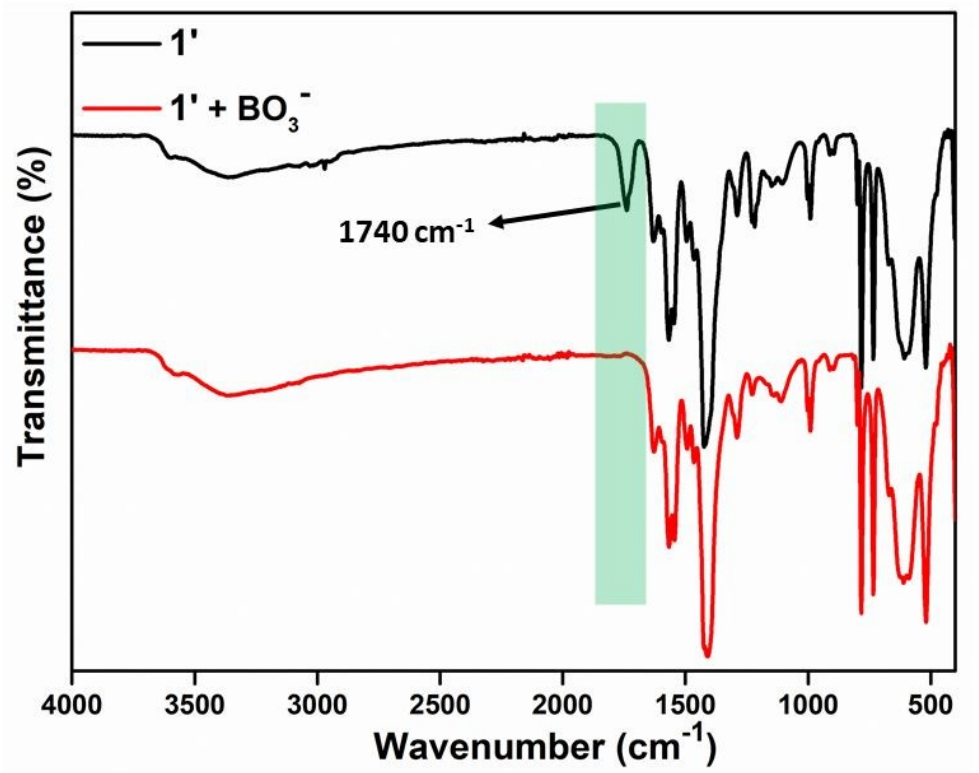

Figure S41. FT-IR spectra of **1′** and perborate-treated **1′** (recovered after sensing).

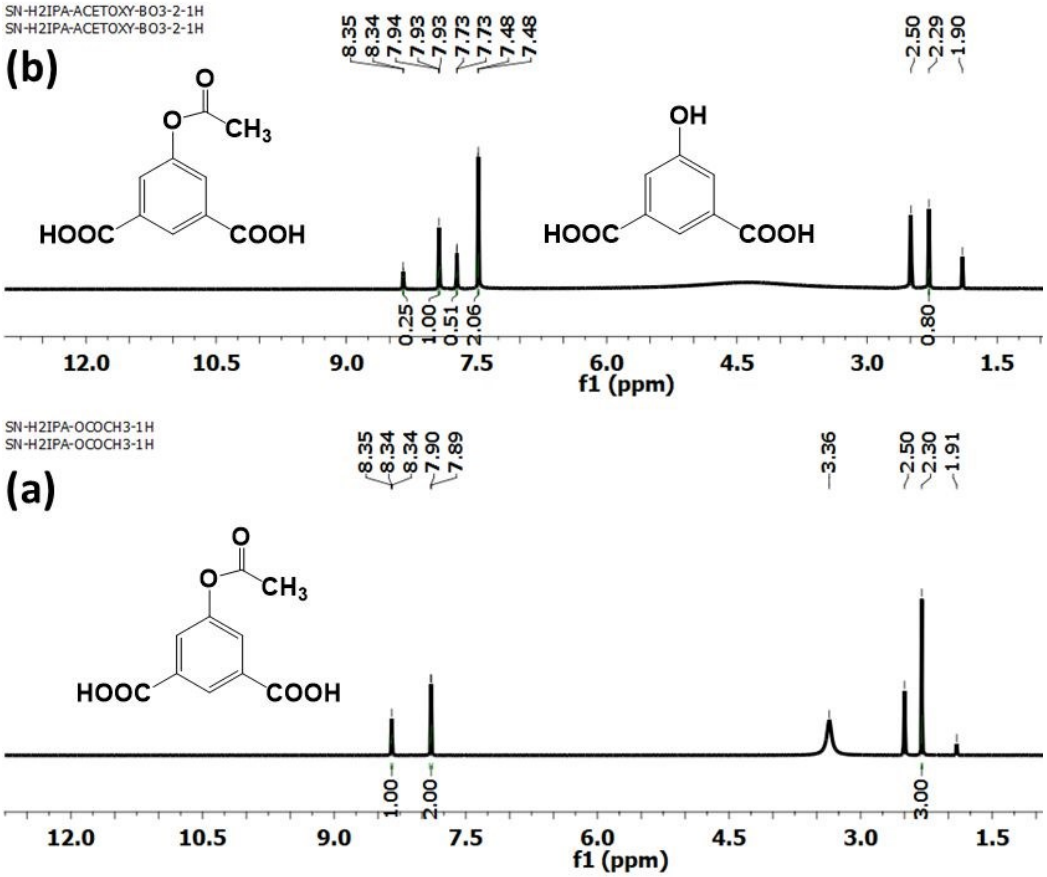

Figure S42. ^{1}H NMR spectrum of (a) H_2IPA-$OCOCH_3$ ligand and (b) perborate-treated H_2IPA-$OCOCH_3$ ligand in DMSO-d_6. New proton signals at 7.93 ppm and 7.48 ppm signify the formation of H_2IPA-OH after treatment with perborate.

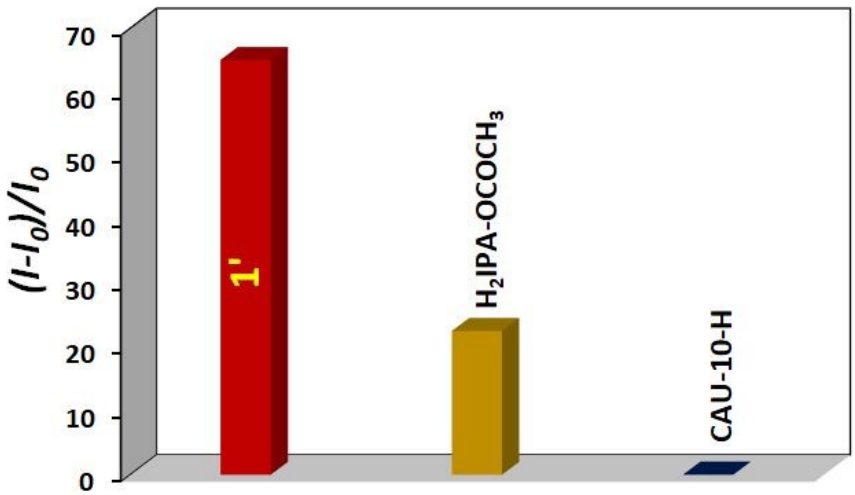

Figure S43. Relative fluorescence response of **1′**, H_2IPA-$OCOCH_3$ ligand and unfunctionalized CAU-10 towards 10 mM $NaBO_3$ (500 μL) in aqueous medium.

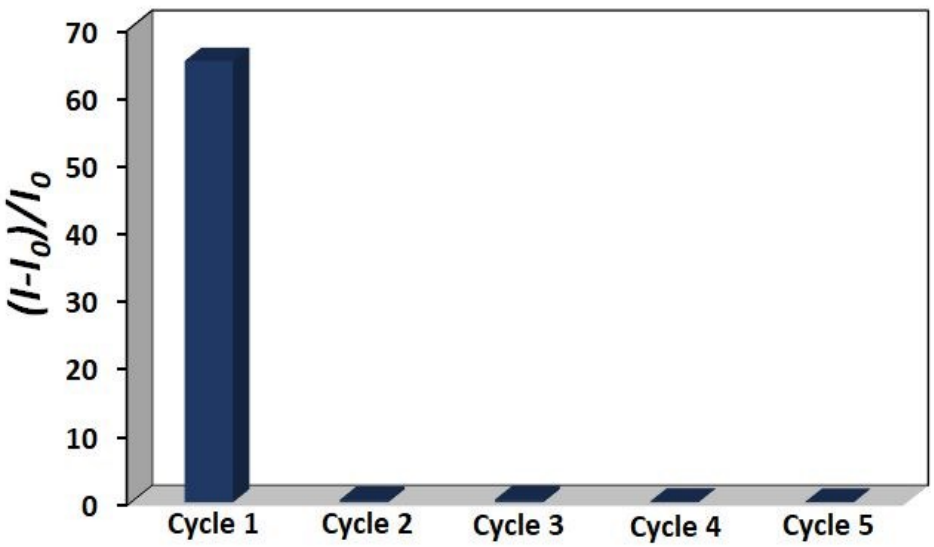

Figure S44. Recyclability test for the fluorescence turn-on response of **1′** towards $NaBO_3$.

Table S2. Comparison of the sensing performance of various fluorescent sensors of perborate.

Sl. No.	Sensor	Type of Material	Sensing Medium	Mode of Detection	Detection Limit	Response Time	Ref.
1	CAU-10-$OCOCH_3$	MOF	water	turn-on	1.19 µM	5 min	this work
2	AIE-perborate	organic-molecule	THF/HEPES (1/99 v/v), pH = 5.0	turn-on	0.10 µM	-	2
3	APBT and ANBT	organic-molecule	(H_2O/CH_3 CN=1:1 v/v, 10 mM HEPES buffer, pH=7.4	ratiometric	9.04 µM and 19.03 µM	90 sec and 110 sec	3
4	compound **1**	organic-molecule	acetate buffer-CH_3CN (90:10, v/v), pH =4.8	turn-on	2.2×10^{-5} M.	5 min	4
5	pyridyl azo-based naphthyl acetate	sol-gel	CH_3CN-H_2O (1:1, v/v)	ratiometric	-	-	5
6	nanosensor **1**	nano-particle	water	turn-on	0.5 µM	-	6

References:

1. J. Liu, Y. Xu, P. B. Groszewicz, M. Brodrecht, C. Fasel, K. Hofmann, X. Tan, T. Gutmann and G. Buntkowsky, *Catal. Sci. Technol.*, 2018, **8**, 5190-5200.
2. R. Zhang, M. Gao, S. Bai and B. Liu, *J. Mater. Chem. B*, 2015, **3**, 1590-1596.
3. A. K. Mahapatra, S. Mondal, S. K. Manna, K. Maiti, R. Maji, S. S. Ali, S. Mandal, M. R. Uddin and D. K. Maiti, *Chemistry Select*, 2016, **3**, 375-383.
4. M. G. Choi, S. Cha, J. E. Park, H. Lee, H. L. Jeon and S.-K. Chang, *Org. Lett.*, 2010, **12**, 1468-1471.
5. A. Panja and K. Ghosh, *Chemistry Select*, 2018, **3**, 9448-9453.
6. R. U. Gawas, S. Anand, B. K. Ghosh, P. Shivbhagwan, K. Choudhary, N. N. Ghosh, M. Banerjee and A. Chatterjee, *Chemistry Select*, 2018, **3**, 10585-10592.